

Cryo-EM Structures of human ABCA7 provide insights into its phospholipid translocation mechanisms

Le Thi My Le^{1†}, James Robert Thompson^{1†}, Sepehr Dehghani-Ghahnaviyeh², Shashank Pant^{2,#},
Phuoc Xuan Dang¹, Jarrod Bradley French¹, Takahisa Kanikeyo³, Emad Tajkhorshid² & Amer
Alam^{1,*}

¹The Hormel Institute, University of Minnesota, Austin, Minnesota 59912

² Theoretical and Computational Biophysics Group, NIH Center for Macromolecular Modeling and Bioinformatics, Beckman Institute for Advanced Science and Technology, Department of Biochemistry, and Center for Biophysics and Quantitative Biology, University of Illinois at Urbana-Champaign, Urbana, IL, USA

³Department of Neuroscience, Mayo Clinic, Jacksonville, Florida 32224

†These authors contributed equally to this work

Current affiliation: Loxo Oncology at Lilly., Louisville, CO 80027, USA

*Address correspondence to: Amer Alam, PhD, aalam@umn.edu

Appendix

Table of contents

Appendix Figure S1. ABCA7_{BPL} characterization and cryo-EM data processing.

Appendix Figure S2. ABCA7_{PE} Cryo-EM data processing.

Appendix Figure S3. ABCA7_{DIGITON} cryo-EM processing.

Appendix Figure S4. ABCA7_{EQ-ATP} cryo-EM processing.

Appendix Figure S5. TMD-ECD interfaces of open and closed form ABCA7.

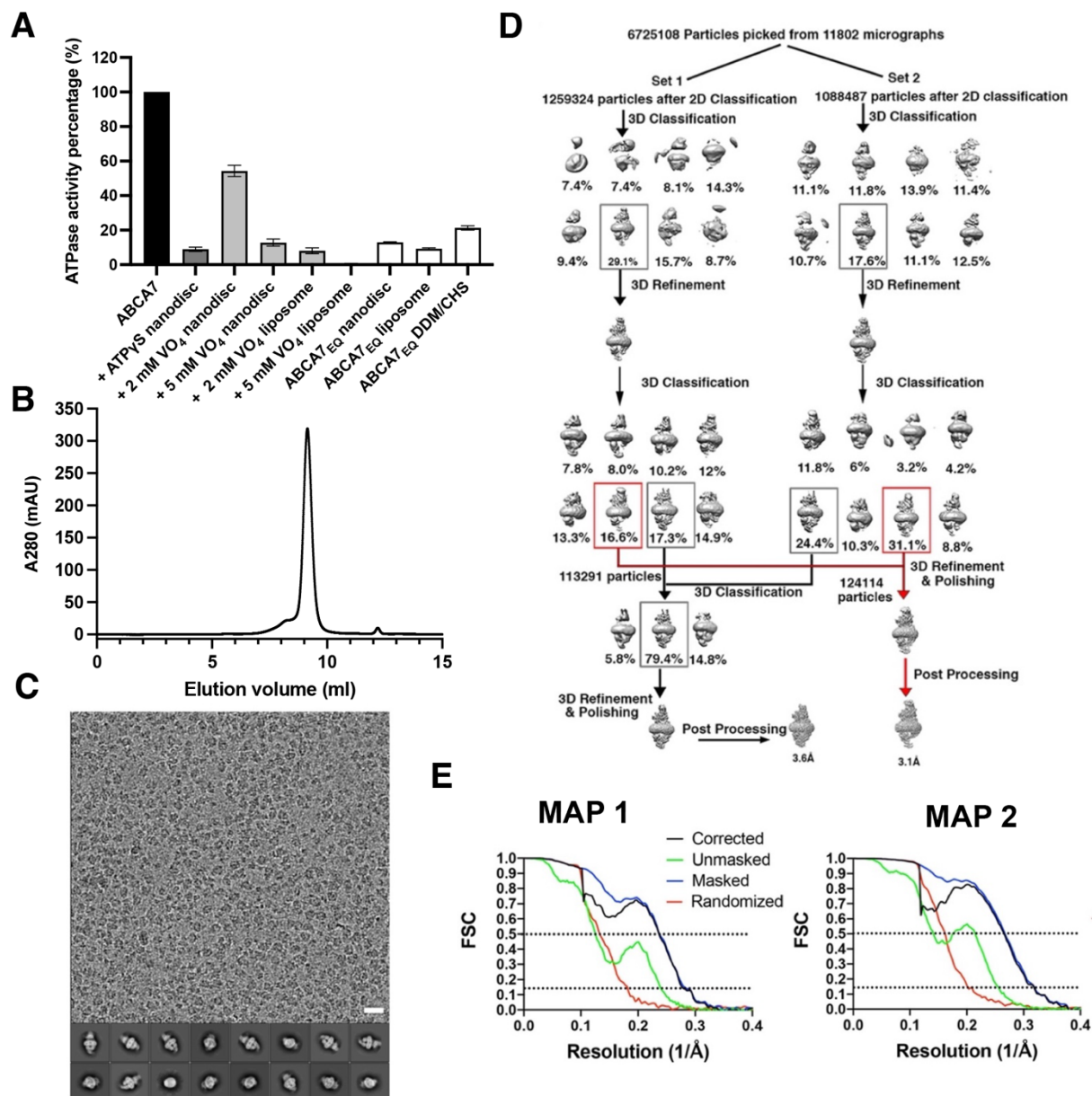
Appendix Figure S6. Histograms of lipid counts in the TMD lumen for POPE and POPC systems.

Appendix Figure S7. Sequence alignment of human (hs) ABCA7, ABCA1, and ABCA4, and ABCA3.

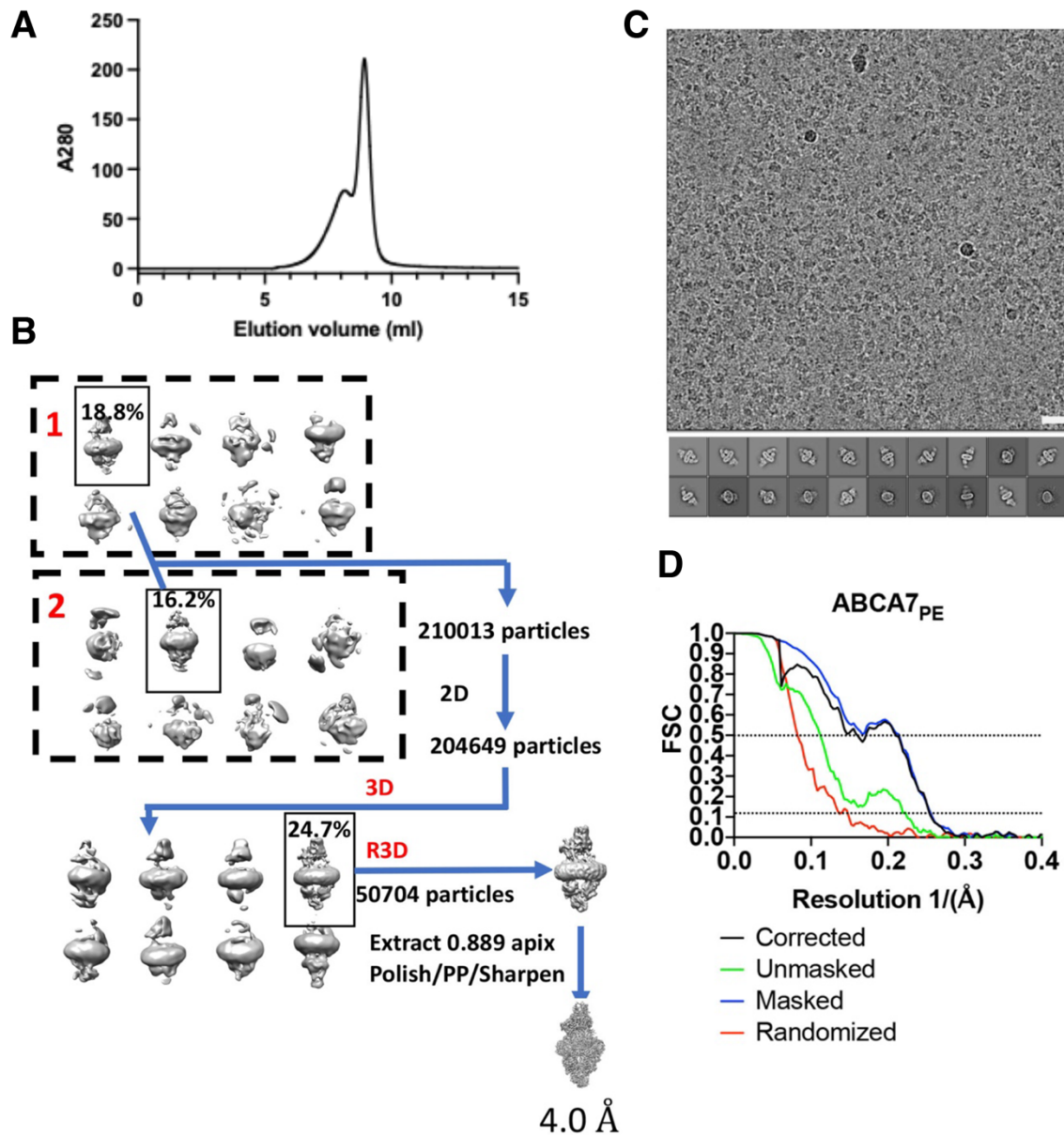
Appendix Figure S8. Amino acid positions of ABCA7 with variants associated with risk of AD.

Appendix Table S1. Table of K_M and V_{Max} values of ABCA7 incorporated in nanodiscs, liposomes, and detergent.

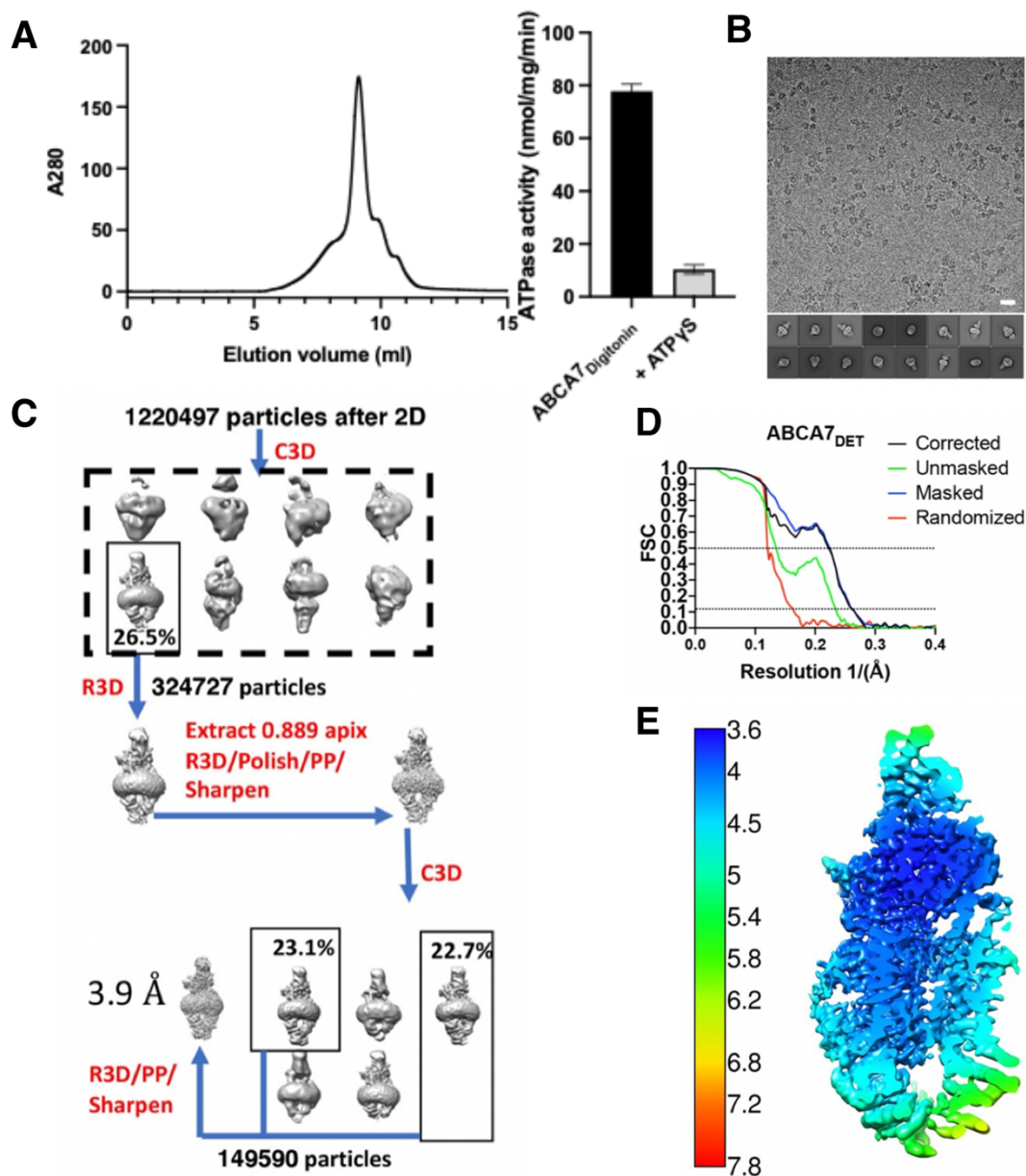
Appendix Table S2. Data collection and refinement statistics.



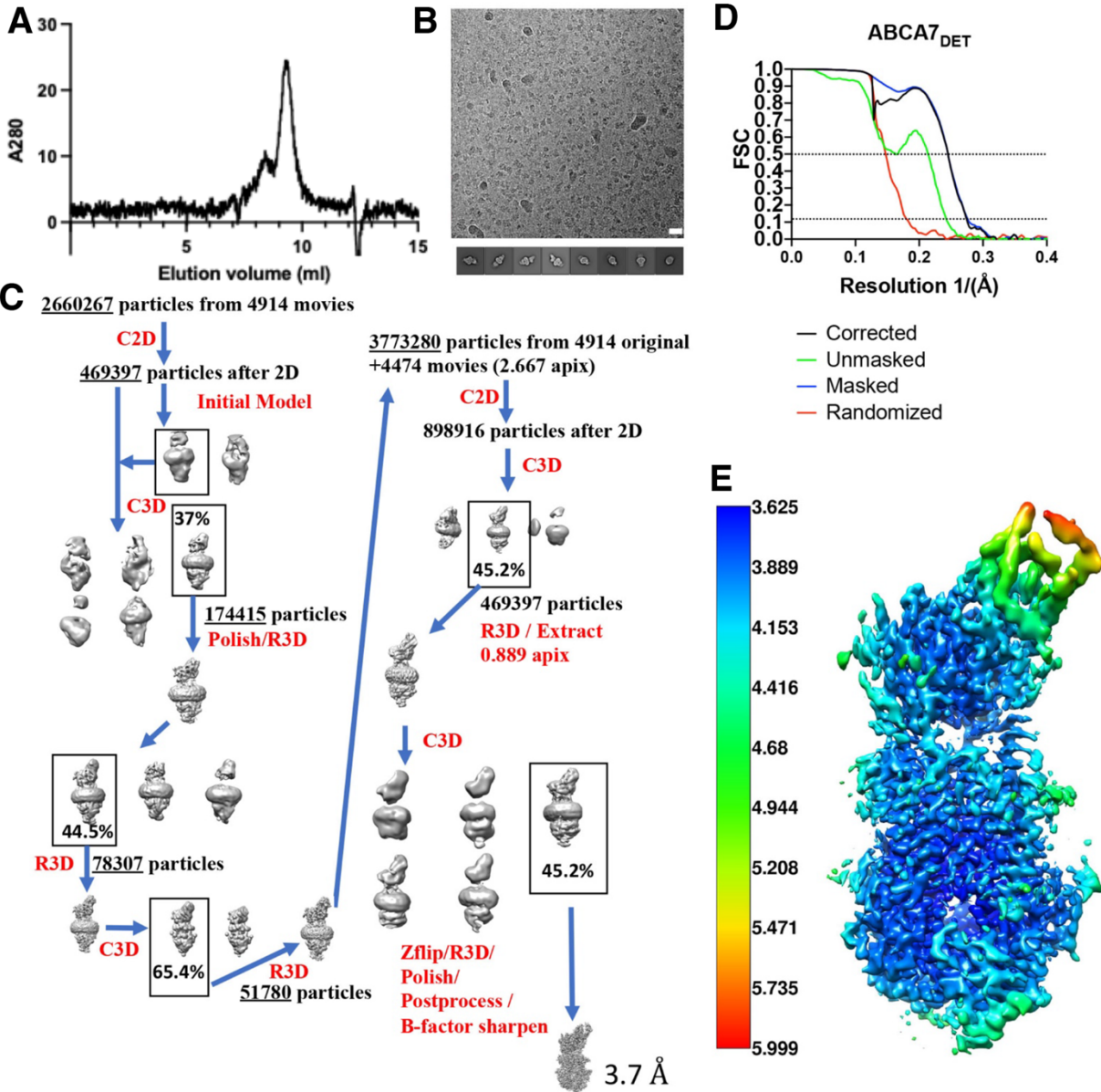
Appendix Figure S1. ABCA7_{BPL} characterization and cryo-EM data processing. (A) ATPase rates for ABCA7 under various experimental conditions as percentage of wildtype ABCA7 ATPase activity in liposomes, nanodiscs, and detergent. ATPase rate comparison for nanodisc and liposome reconstituted ABCA7 with and without ATP analog adenosine-5'-o-(3-thio-triphosphate) (ATP γ S) or sodium orthovanadate (VO $_4$) along with a hydrolysis-deficient mutant ABCA7_{EQ} in nanodiscs, liposomes, and detergent. Experimental replicates (n)=3 and error bars represent standard deviation (s.d). (B) SEC peak of ABCA7_{BPL} samples for cryo-EM. (C) Representative cryo-EM micrograph at -2.5 μ m defocus. Scale bar = 20 nm. (D) cryo-EM processing workflow. Boxes indicate 3D classes used for further refinement for both Map 1 and Map 2 (red). (E) Fourier shell correlation (FSC) curves for Map 1 (top) and Map 2 (bottom) Dotted lines indicate position 0.143 and 0.5 cutoff criteria for resolution estimates.



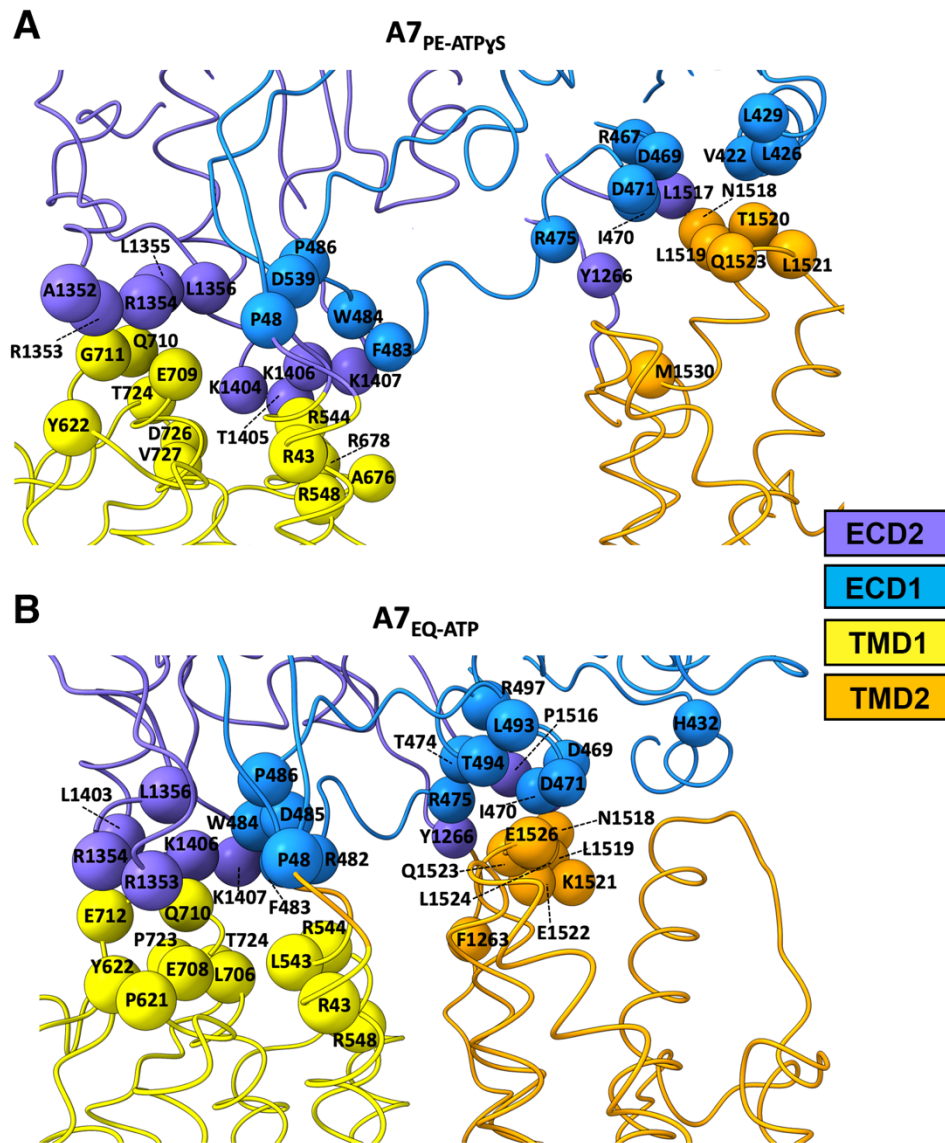
Appendix Figure S2. ABCA7_{PE} Cryo-EM data processing. (A) Size exclusion chromatography micrograph of cryo-EM sample showing monodisperse ABCA7_{PE} nanodisc (main peak). (B) Representative micrograph at -2.5 μm defocus and 2D classes. Scale bar = 20 nm. (C) cryo-EM processing workflow. Dashed boxes demarcate Subsets 1 and 2. Solid boxes indicate 3D classes used for further refinement. 2D = 2D Classification, 3D = 3D classification, R3D = 3D refinement. (D) Fourier shell correlation (FSC) curves for ABCA7_{PE}. Dotted lines indicate position 0.143 and 0.5 cutoff criteria for resolution estimates.



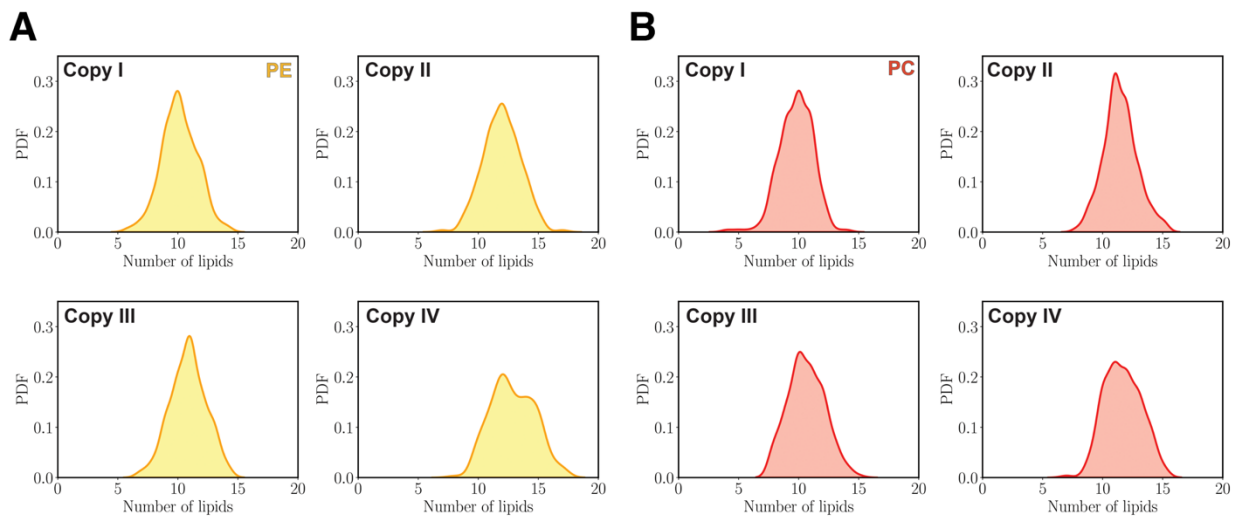
Appendix Figure S3. ABCA7^{DIGITONIN} cryo-EM processing. (A) SEC profile of ABCA7^{DIGITONIN} and its ATPase activity with and without ATPγS. (B) Representative micrograph at -2.5 μm defocus and 2D classes. Scale bar = 20 nm. (C) cryo-EM processing workflow. C2D = 2D Classification, C3D=3D classification, R3D = 3D refinement. (D) Local resolution colored EM map of ABCA7^{DIGITONIN}. (E) Fourier shell correlation (FSC) curves for ABCA7^{DIGITONIN}. Dotted lines indicate position 0.143 and 0.5 cutoff criteria for resolution estimates.



Appendix Figure S4. ABCA_{7EQ-ATP} cryo-EM processing. (A) SEC peak for ABCA_{7EQ-ATP} in nanodiscs. (B) Representative EM micrograph (-2.5 defocus) and rep 2D classes for ABCA_{7EQ-ATP} sample. © Cryo-EM data processing pipeline. C2D = 2D Classification, C3D=3D classification, R3D = 3D refinement. (D) FSC curves for ABCA_{7EQ-ATP}. Dotted lines indicate position 0.143 and 0.5 cutoff criteria for resolution estimates. (E) Local resolution colored EM map.



Appendix Figure S5. TMD-ECD interfaces of open and closed form ABCA7. (A) The TMD-ECD binding interfaces of ABCA7_{PE} with TMD1 and TMD2 and with C α for residues in TMD1 and TMD2 within 5 Å of either ECD or vice versa shown as spheres. (B) The same analysis for the TMD-ECD binding interfaces of ABCA7_{EQ-ATP} with closed cavity.



Appendix Figure S6. Histograms of lipid counts in the TMD lumen for POPE and POPC systems. (A/B) POPE and POPC lipid counts in the lumen of ABCA7 captured through the 2 μ s of MD simulations. The histograms were calculated for each protein's copy separately and shown here. Y-axis of the histograms represent probability distribution function (PDF). Copy IV of the POPE system shows more lipid penetration to the lumen of TMD compared to other POPE and POPC systems.

```

1      10      20      30      40      50      60      70      80      90
ABCA7 MAFWTLQLLLLWKNFMYRRRQPVQLVLELLWPLFLLFLLVAVRHSHPLEHHECHFPNKLPSAGVPWLQGLCNVNNTCPVQLTPGEPFG
ABCA1 MACWPLQLLLLWKNLTFRRRQTCQLLLEVAVPLFLLFLLVLSVRLSYPPYEHHECHFPNKLPSAGLPWVQGIICNANNPCVRYPTPGEPAPG
ABCA4 MGFVVRQILLLWKNWTLRRRQKIRFVVELWPLSLFLLVLLWLNANPLYSHECHFPNKLPSAGLPWVQGIICNANNPCVQSPTPGEPSPG
ABCA3 .....

100    110    120    130
ABCA7 RLSNFNDSLVSRLLADARTVLLGGASAHRTLAGLGLKLTATLRA.....ARSLTAQPQPTK
ABCA1 VVGNFNKSIVARLIFSARRLLLYSQKDTSMKDMRKVLRLLTQQI.....KKSSSNLKLQDFLVDNETFSGLYHNLSLPKSLTVDKMLRA
ABCA4 IVSNNNSILARVYRDFQELLMNAPESQHLGRITWTEHLHLISQFMDLIRTHEPERIAGRIRIRIDLKDEETLTLFLIKNIGLSDSVVYLLINS
ABCA3 .....

150    160    170    180
ABCA7 QSPLEPPMLDVAEELITSLRTESEL.....GALGQAQ.....EPLHS
ABCA1 DVILHKVFLQGGQLHLITSLCNGSKSEEMIQLDGQEVSE.....LCLLPREKLAARVLRNSMMDILKPLRLTINSTSPFPKELAEATKT
ABCA4 QVRPEQFAHGVPDLALKDIACSEALLERFIIFSQRRAKTVRYALCSLQSGTLQWIEDTLYANVDFFKLFRVLPPTLLDSRQGINLRSGG
ABCA3 .....

190    200    210    220    230    240    250    260
ABCA7 LLEALEDLAEQLLALRSLVLELRALLQRFRGTSGP.....LELLESALCSVVRGFSSTVGPSTLWYEA...SMLMELVQ...QEPESALPDSLSL
ABCA1 LLLHSLGTLAEQLFSMRSSWSDMRQEVMLFTNVNSSSSSTQIYQAVSRIVCGHPEGGGLKIKSLWYEDNNYKALFGNGTTEEDAETFYDNST
ABCA4 ILLSDMSPRIQELIHRSSMODLLWVTRPLMNQGGPETFTFLMGFLSLLCGLYPEGGSRVLSFNWYEDNNYKAFGLIDSTRKDPISYDRRT
ABCA3 .....

270    280    290    300    310    320    330    340    350
ABCA7 PACSELIQALDISHPLSRLLRWRKPLILGKIDFAFDPTFTRKLMQVNRTFEELTLLRDVRVWEMLGPRIFTLMDNDSNVAMLQRLQMQD
ABCA1 SFYCNALIKSLESPLSRKIWRKAPLVLGKIDYTPDTPATROVMAEYKTFQELAVFHDLEGMWELSPKIWTMENESQEMDLVRMLLDSRD
ABCA4 PFCNALIQELIHRSSMODLLWVTRPLMNQGGPETFTFLMGFLSLLCGLYPEGGSRVLSFNWYEDNNYKAFGLIDSTRKDPISYDRRT
ABCA3 ..MALLVRLQALDISHPLSRLLRWRKPLILGKIDFAFDPTFTRKLMQVNRTFEELTLLRDVRVWEMLGPRIFTLMDNDSNVAMLQRLQMQD

360    370    380    390    400    410    420    430
ABCA7 EGRQRPRFGGRDHML...EALRSFLDPG.....SGGYSWDAHADVGHVGTGRVTECLSDKLEAAPSAAALVSRALQLLAEHRFWAGV
ABCA1 NDHFWEQQLDGLDWTAAQDVAFLAKHPEDVQSSNGSVYWRERAFNETNQARTIRSRFMECVNLNKLKLEPIATEVWLLINKSMELLDKRFKFWAGI
ABCA4 VKDFLNRQLGEEGITAEALNLFYKGPRESQADDMANFYWRERAFNETNQARTIRSRFMECVNLNKLKLEPIATEVWLLINKSMELLDKRFKFWAGI
ABCA3 AAKTVTEVRRALVINMRVRF.....PSEKDEEDYIRYDNCSSVLAAVVEHPEHNSKEPLPLAVKYHLRFSYTRRNYMFTQ.

440    450    460    470    480    490    500    510    520    530
ABCA7 VFLGPESSDPTHEPTPDLGPGHVIKIRMDIDVIVRTNKIRDRFWDPGPAADPLTDLRYVWGGFVYLDLVBRAAVRVLSGANPRAGLYLQ
ABCA1 VF.....TGITPGSIELPHVVKYKIRMDIDNVEVRTNKIRDRYWDPGPRADPFEDMRYVWGGFAYLQDVBQAITIRVLTGTEKTKGVYMQ
ABCA4 VFLGPESSDPTHEPTPDLGPGHVIKIRMDIDVIVRTNKIRDRYWDPGPRADPFEDMRYVWGGFAYLQDVBQAITIRVLTGTEKTKGVYMQ
ABCA3 ..L.....TGSEFLKETEGRHTTSLFFLFPNPGFREPSTPDG.GEPCYIRREGFLAVQH....AVDRAIMVYHADAAATROQLFQRLTVTIK

540    550    560    570    580    590    600    610
ABCA7 QMPYPYCYVDVDFHRLVRSRSLPLFTLAWIYVSVTLTKAVVVEKEKTRLDTRMRAMGSRVAVLWLGWFLSCLGPFLLSAAALLVVLKLG....
ABCA1 QMPYPYCYVDVDFHRLVRSRSLPLFTLAWIYVSVTLTKAVVVEKEKTRLDTRMRAMGSRVAVLWLGWFLSCLGPFLLSAAALLVVLKLG....
ABCA4 QMPYPYCYVDVDFHRLVRSRSLPLFTLAWIYVSVTLTKAVVVEKEKTRLDTRMRAMGSRVAVLWLGWFLSCLGPFLLSAAALLVVLKLG....
ABCA3 RFYPYPIADPFHRLVRSRSLPLFTLAWIYVSVTLTKAVVVEKEKTRLDTRMRAMGSRVAVLWLGWFLSCLGPFLLSAAALLVVLKLG....

620    630    640    650    660    670    680    690    700
ABCA7 DILTPYSHGQVVFVFLAAFAVATVTSQSLLSAFFFSRANLAAACGGLAYFSVYHPVYLCVAVRDRLPAGGRVAAALLSPVAFGGCGESLALLEE
ABCA1 NLLYSDSFFVVFVFLAAFAVATVTSQSLLSAFFFSRANLAAACGGIYFTVYHPVYLCVAVRDRLPAGGRVAAALLSPVAFGGCGEYFALRE
ABCA4 RILHYSDSFFLFLFLAAFAVATVTSQSLLSAFFFSRANLAAACGGIYFTVYHPVYLCVAVRDRLPAGGRVAAALLSPVAFGGCGEYFALRE
ABCA3 AVLSRSDSFLVLAFLAFAVATVTSQSLLSAFFFSRANLAAACGGIYFTVYHPVYLCVAVRDRLPAGGRVAAALLSPVAFGGCGEYFALRE

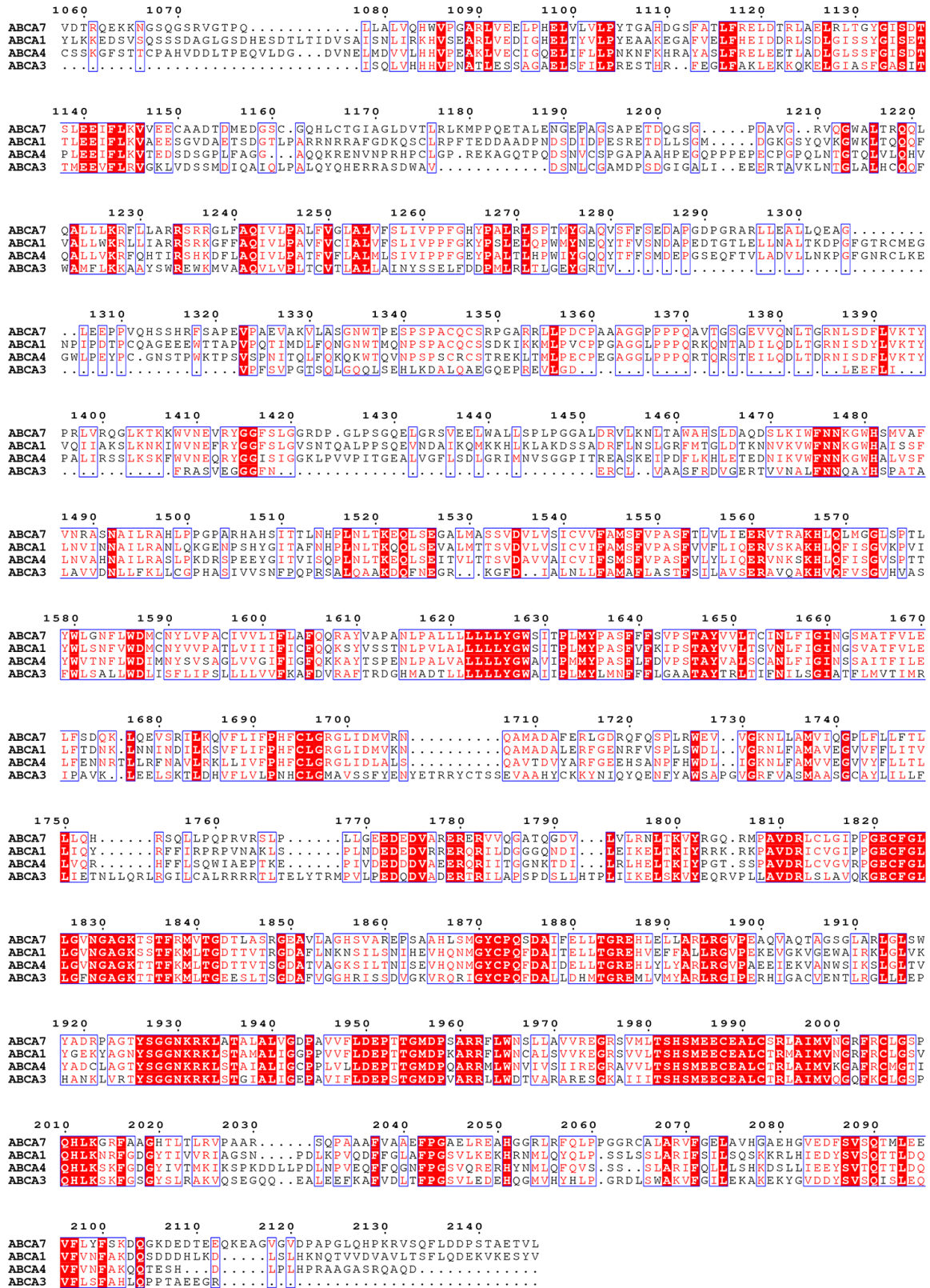
710    720    730    740    750    760    770    780    790
ABCA7 CGEGAQWNVGTRPTADVFSLAQVSGLLLDALYGLATWYLEAVCPGOYGPDPWNPFPRRSYWG.....PRPPKSPACPPTLDD.
ABCA1 CGIGVQWNVGTRPTADVFSLAQVSGLLLDALYGLATWYLEAVCPGOYGPDPWNPFPRRSYWG.....PRPPKSPACPPTLDD.
ABCA4 CGIGVQWNVGTRPTADVFSLAQVSGLLLDALYGLATWYLEAVCPGOYGPDPWNPFPRRSYWG.....PRPPKSPACPPTLDD.
ABCA3 KGMCHQWRDLSPVNVDDDFCFQVLLMLLDALYGLATWYLEAVCPGOYGPDPWNPFPRRSYWG.....PRPPKSPACPPTLDD.

800    810    820    830    840    850    860    870
ABCA7 .....PKVLYVEAPPGVSVRSIEKRF...GSPQFALRGLSLDFYQGHITAFGLHNGAGKTTLSLSCGLFPPSGSFAFLLGHVYRS
ABCA1 .....ISEICMBEETHLKLGVSIQNDVKVYR...DGMKAVDGLALNFYEGQITRFLHNGAGKTTTMSLTLGLFPPTSGTAYILGKDIRS
ABCA4 PEHPGFIHDSFPERHPGMVPGVCKNIVKIFE...PCGRPAVDRLNITFYENQITAFGLHNGAGKTTTMSLTLGLFPPTSGTAYILGKDIRS
ABCA3 .....KALRNEYFPAEEDLVA...KIKHHSKVRVGNKDRAAVDRLLNLNLYEGQITVFLGHNGAGKTTTMSLTLGLFPPTSGRAYISGYEISQ

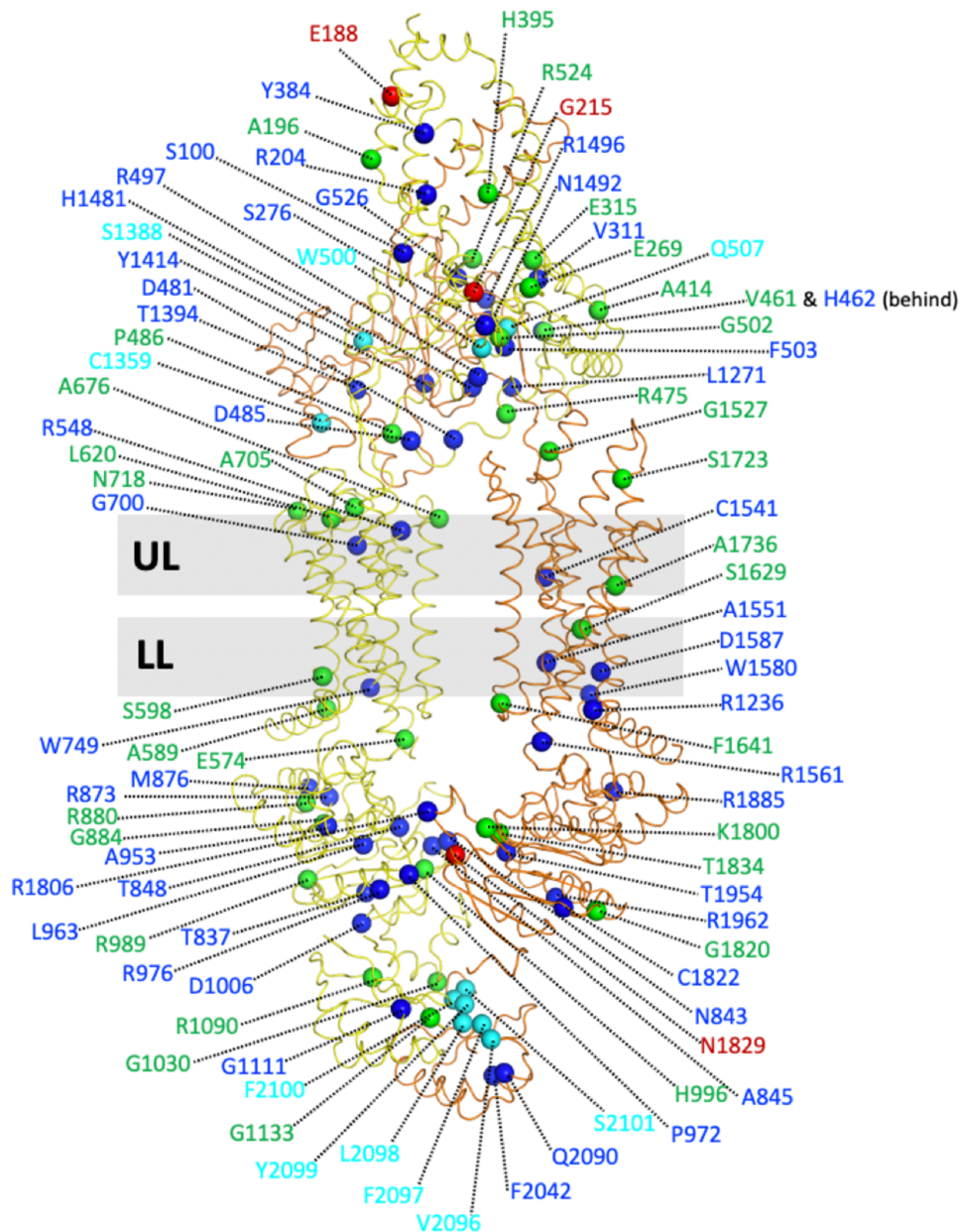
880    890    900    910    920    930    940    950    960
ABCA7 SMAATRPILGVCPOYNVLFDMLTVDHEHWVYGRKLGLSAAVVGPEQDRLLQDVGTVSRSQSVQTRHLSGGMORKLSVAIAFVGGSDVILDE
ABCA1 EMSTIRONLGVCPQHNVLFDMLTVDEHHLWVYGRKLGLSAAVVGPEQDRLLQDVGTVSRSQSVQTRHLSGGMORKLSVAIAFVGGSDVILDE
ABCA4 SLDVAVRQSLGMCPQHNILFHHLTVAEHMLFYAQLKGLSQEAAQLEMALEDTG...HRRNEEAQDLSGGMORKLSVAIAFVGGSDVILDE
ABCA3 DMVQIRKSLGICPOHDLIFNLTVAEHLVYFAQLKGLSRQKCPPEVQRKMLHIGH...EDKWNRSRFLSGGMORKLSVIGIALIAGSRVILDE

970    980    990    1000  1010  1020  1030  1040  1050
ABCA7 PTAGVDPASRRGTWELLKYREGRTLILSTHLLDDEAELLDGRRVAVAGGRVCCCGSPLFLRRLHLSGYYITLVKARLPLITTEKADTDMEGS
ABCA1 PTAGVDPYSRRGTWELLKYRQGRITILSTHLLDDEADVLGDRVAIISHGKIVCCCGSPLFLRRLHLSGYYITLVKARLPLITTEKADTDMEGS
ABCA4 PTAGVDPYSRRGTWELLKYRSGRTIIMSTHLLDDEADVLGDRVAIISHGKIVCCCGSPLFLRRLHLSGYYITLVKARLPLITTEKADTDMEGS
ABCA3 PTCGMDATSRRAITWLLQKSDRTIVLTTHEMDEADVLGDRVAIISHGKIVCCCGSPLFLRRLHLSGYYITLVKARLPLITTEKADTDMEGS

```

Appendix Figure S7. Sequence alignment of human (hs) ABCA7, ABCA1, and ABCA4, and ABCA3.



Appendix Figure S8. Amino acid positions of ABCA7 with variants associated with risk of AD. Structure of ABCA7 with C α atoms shown for amino acid with known pathogenic variants (green), protective variants (red), and ABCA7 residues conserved in ABCA1 with mutations known to disrupt the latter's binding to apoA1 and/or phospholipid translocation (blue). Cyan spheres highlight residue positions of ABCA1 mutations known to disrupt phospholipid efflux including those equivalent to the VFVNFA motif within the ABCA1 RD. Grey bars indicate the upper (extracellular) and lower (cytoplasmic) membrane bilayer leaflets (UL and LL, respectively).

	Nanodiscs	Detergent (DDM/CHS)	Liposomes
K_M	0.51	0.43	0.74
V_{Max}	37.41	162.9	167.8

Appendix Table S1. Table of K_M and V_{Max} values of ABCA7 incorporated in nanodiscs, liposomes, and detergent.

Dataset	ABCA7 _{BPL}		ABCA7 _{PE}	ABCA7 _{DIGITONIN}	ABCA7 _{EQ-ATP}
Magnification	96k		96k	96k	96k
Pixel Size (Å)	0.895		0.889	0.889	0.89
Total Dose (e/Å ²)	60		40	40	40
Defocus Range (um)	-0.8 to 2.6		-0.8 to 2.6	-0.8 to 2.6	-0.8 to 2.6
Maps	Map 1	Map 2	Map3		
EMDB ID	EMD-28041	EMD-28044	EMD-28047	EMD-28050	EMD-28451
# Particles in final Class	91381	124114	50704	149590	177230
Resolution (Å) (0.143 threshold)	3.6	3.2	4.0	3.9	3.7
Sharpening B factor	-82.9	-20	-132	-50	-134.1
Refined Coordinates	ABCA7 _{BPL}		ABCA7 _{PE}	ABCA7 _{DIGITONIN}	ABCA7 _{EQ-ATP}
PDB ID	8EDW		8EE6	8EEB	8EOP
# Residues/Non-hydrogen Atoms	1804/14311		1808/14475	1873/14673	1687/13266
Ligands	20		26		4
R.M.S deviations					
Bond Length (Å)	0.003		0.003	0.002	0.003
Bond Angles (°)	0.676		0.683	0.626	0.593
MolProbity Statistics					
MolProbity Score	1.76		1.69	1.73	1.76
Clashscore	8.80		8.30	9.05	6.82
Poor rotamers (%)	0.07		0.07	0.00	0.00
Ramachandran statistics					
Favored (%)	95.80		96.42	96.61	94.30
Allowed (%)	4.14		3.52	3.39	5.64
Outliers (%)	0.06		0.06	0.00	0.06

Appendix Table S2. Data collection and refinement statistics.